

# Pion Form Factor and Quark Mass Evolution in a Light-Front Bethe-Salpeter Model

L. S. Kisslinger<sup>a</sup>, Ho-Meoyng Choi<sup>a</sup> and Chueng-Ryong Ji<sup>b</sup>

<sup>a</sup>*Department of Physics, Carnegie-Mellon University, Pittsburgh, PA 15213*

<sup>b</sup>*Department of Physics, North Carolina State University, Raleigh, NC 27695-8202*

(October 24, 2018)

We discuss the soft contribution to the elastic pion form factor with the mass evolution from current to constituent quark being taken into account using a light-front Bethe-Salpeter (LFBS) model, which is a light-front quark model (LFQM) with a running mass. It is shown that partial conservation of the axial-vector current (PCAC) is satisfied with a running quark mass. We examine the sensitivity of the pion form factor using two different functional forms of the quark propagator. The Ball-Chiu ansatz is used to maintain local gauge invariance of the quark-photon vertex. The extension of our model to the hard contribution is also discussed.

PACS numbers: 12.39.Ki, 13.40.Gp, 14.40.Aq, 14.40.Lb

## I. INTRODUCTION

The pion electromagnetic (EM) form factor is of great interest for the study of Quantum Chromodynamics (QCD). At low momentum transfers ( $Q^2$ ) nonperturbative QCD (NPQCD) dominates, while at large  $Q^2$  perturbative QCD (PQCD) can be used to calculate the asymptotic form factor; and the transition from NPQCD to PQCD has long been of interest [1]. Since PQCD can only be used for  $Q^2 > 1 \text{ GeV}^2$ , light-front (LF) quantization methods may be most useful [2]. In the early work on the pion form factor [3] using the light-front Bethe-Salpeter equation (LFBSE) [4] the NPQCD (soft) part was separated from the PQCD (hard) part; and it was shown in a model calculation that the transition from NPQCD to PQCD is expected in the region  $5.0 < Q^2 < 15.0 \text{ GeV}^2$ . This work was extended [5] to include the Sudakov form factor [6], anomalous quark magnetic dipole moments, and a simple model for the running quark mass,  $m(Q^2)$ . Improved calculations of the pion EM form factor are motivated by the recent new and upgraded data (up to  $Q^2=1.6 \text{ GeV}^2$ ) from the Jefferson Laboratory (JLab) [7]. While this  $Q^2$  range may be too low to determine the transition to the PQCD region, these data are useful for studying NPQCD theoretical approaches. In the present work we restrict ourselves to the soft NPQCD part with models for the running mass that ensure gauge invariance and consistency with the partially conserved axial current (PCAC) relation [8]

$$m_\pi^2 f_\pi = -2m_{(\nu)} \langle 0 | \bar{q} \gamma_5 q | \pi \rangle_{(\nu)} = -2m_{(\nu)} \frac{\langle \bar{q} q \rangle_{(\nu)}}{f_\pi}, \quad (1)$$

where  $m_{(\nu)}=m_0$ (current mass) in spacelike  $p^2=\nu^2$  region( $\nu$  is the renormlization point) and  $\langle \bar{q} q \rangle_{(\nu)}$  is the

quark condensate.

Since we are only considering the soft part of the pion form factor here, the LFBS amplitude can be modeled by a light-front wave function [9] based on LF Hamiltonian dynamics, such as the light-front constituent quark model(LFCQM) [10–12], but an essential ingredient is the use of a running quark mass, which is the main subject of the present paper. In LF quantization, a possible connection is anticipated between the constituent quark model(CQM) and QCD due to the rational energy-momentum dispersion relation that leads to a relatively simple vacuum structure. There is no spontaneous creation of massive fermions in the LF quantized vacuum. Thus, one can immediately obtain a constituent-type picture, in which all partons in a hadronic state are connected directly to the hadron instead of being simply disconnected excitations (or vacuum fluctuations) in a complicated medium. In particular, a systematic program has been laid out in the calculation of the space-like EM form factor of pseudoscalar mesons because only parton-number-conserving Fock state (valence) contribution is needed when the “good” components of the current,  $J^+(=J^0+J^3)$  and  $J_\perp=(J_x, J_y)$ , are used in the Drell-Yan-West( $q^+=0$ ) frame [13,4]. The new data from the JLab [7] seem to be in good agreement with the previous CQM result [12] based on a QCD-motivated linear confining potential. However, a possible realization of chiral symmetry breaking in the LF vacuum is an underdeveloped aspect of LF quantization.

In contrast to quark models or LFCQM which use a phenomenological constant constituent quark mass, an approach based on QCD quantum field theory is the Bethe-Salpeter (BS) equation in conjunction with Dyson-Schwinger (DS) equations for the quark propagators, gluon propagator and vertices. We note an important result of recent DS calculations, in which the effective running mass,  $m(p^2)$ , is calculated [14]. In these DS calculations the parameters for model gluon propagators are fixed by fitting the quark condensate, the mixed condensate and even the form of the nonlocal condensate [15]. It is particularly interesting to note that the DS quark propagator with running masses that decrease with respect to  $p^2$  faster than quark models gives properties of the rho [16] and pion [17] that are in agreement with experiment. In all of these DS calculations it has been found that the effective quark mass drops very rapidly with increasing  $Q^2$ . Since the covariant BS/DS approach and the LF approach are not same but complementary, it may be necessary to examine if the previous LFCQM

result [12] is intact even if the quark mass evolves as rapid as BS/DS approach found. This is a strong motivation for reformulating the LFCQM with a running quark mass, which we do in the present work.

In the present work, we analyze the effect of the mass evolution (from constituent to current quark mass) on the elastic pion form factor at low and intermediate  $Q^2$ . A correct theoretical approach to such a study is the LFBSE coupled to LFDS equations. From the LFDS equations the running quark mass is obtained from the dressed quark propagator. Although the LFDS equation has recently been developed [18], only simple model solutions are available, and here we use a parameterization of the running quark mass that is consistent with known observations. While the asymptotic behavior of the running mass might require the crossing symmetry (under  $Q^2 \leftrightarrow -Q^2$ ) at high momentum  $Q^2$  analogous to that of pion form factor, there is no clue yet for the small momentum behavior in timelike region. Thus, we present the two different forms of mass evolution function; one is crossing asymmetric and the other is crossing symmetric. We then compare the results for the two cases. It should be noted that the recent LFDS results [18] also show a rapid decrease of effective quark mass with momentum that puts the use of quark models for calculating any but static properties in question. In the present work we use forms for the quark mass evolution that are consistent with conventional quark models for calculating hadronic properties at momentum transfers less than about 800 MeV.

The paper is organized as follows: In Sec. II, we review the formulation that underlies a description of the elastic pion form factor within a modeling of QCD through the LFBSE, which is a LFQM with a running mass. In Sec. III, we formulate the running quark mass in LF framework and discuss the local gauge invariance at the quark-photon vertex, i.e. Ward-Takahashi identity [19], due to the momentum dependent quark propagator. In Sec. IV, we analyze the running mass effect on the pion form factor, charge radius, and decay constant obtained from the previous CQM [12] calculation. We also show that our model with the running quark mass is consistent with the PCAC relation given by Eq. (1). This simply means that we obtain a quark condensate consistent with the phenomenological value given in Eq. (1), which is true in the DS calculations [14,15]. A conclusion follows in Sec. V.

## II. MODEL DESCRIPTION

The LFBSE introduced in Refs. [3,5] has the form

$$\Psi(x, \mathbf{k}_\perp) = \int [dy][d^2\mathbf{l}_\perp] \left[ \mathcal{K}_c(x, \mathbf{k}_\perp; y, \mathbf{l}_\perp) + \mathcal{K}_g(x, \mathbf{k}_\perp; y, \mathbf{l}_\perp) \right] \Psi(y, \mathbf{l}_\perp), \quad (2)$$

where  $\mathcal{K}_g$  is the gluon exchange kernel and  $\mathcal{K}_c$ , the difference between the complete BS kernel and  $\mathcal{K}_g$ , includes all confining effects. These kernels were obtained from the relativistic string and LF perturbative QCD (PQCD), respectively. Since NPQCD has not yet provided a form for the confining kernel, in Ref. [5] the problem of solving for the complete BS amplitude,  $\Psi(x, \mathbf{k}_\perp)$ , was avoided by using a model for the soft amplitude. I.e., the soft BS amplitude,  $\Psi^s(x, \mathbf{k}_\perp)$ , can be considered to be the solution of the equation

$$\Psi^s(x, \mathbf{k}_\perp) \equiv \int [dy][d^2\mathbf{l}_\perp] \mathcal{K}_c(x, \mathbf{k}_\perp; y, \mathbf{l}_\perp) \Psi^s(y, \mathbf{l}_\perp). \quad (3)$$

Iterating Eq. (2) by inserting  $\Psi^s$  for  $\Psi$ , one obtains the approximate form

$$\Psi(x, \mathbf{k}_\perp) \approx \Psi^s(x, \mathbf{k}_\perp) + \int [dy][d^2\mathbf{l}_\perp] \mathcal{K}_g(x, \mathbf{k}_\perp; y, \mathbf{l}_\perp) \Psi^s(y, \mathbf{l}_\perp). \quad (4)$$

This BS amplitude contains both soft and hard ingredients needed to take care of momentum transfer for all  $Q^2$  therefore is correctly characterized as including both confinement and asymptotic features of a composite quark system. This approach to the pion form factor has been shown [5] to be in good agreement with the direct BS calculation [3], and to converge rapidly. The extension of Eq. (3) to the non-wave-function vertex in the particle-number-nonconserving Fock state contribution has recently been discussed in Ref. [20].

One nice feature of this approach is that one determines the soft part and the hard part separately, so that one can determine the transition from soft to hard QCD within this LFBS approach. This will be the subject of our future work. For the present work of low- and medium- $Q^2$ , we only consider the confining part of the BS amplitude. We thus may be able to use the LFCQM, which has included many important properties of the  $Q^2$  range that we focus in this work. Therefore, in the rest of this work we use the LF wave function for the LFBS amplitude.

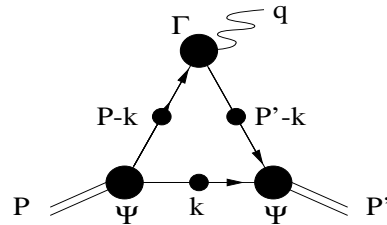


FIG. 1. The valence diagram with dressed quark propagators for the pion EM form factor calculation in  $q^+ = 0$  frame where  $p_q = P - k$ ,  $p'_q = p_q - q = P' - k$  and  $p_{\bar{q}} = -k$ .

The elastic pion form factor is related to pion EM current by the following equation

$$\langle P' | J^\mu(0) | P \rangle = (P' + P)^\mu F_\pi(Q^2). \quad (5)$$

As usual, our calculation will be carried out using the  $q^+ = 0$  frame where  $q^2 = (P - P')^2 = q^+q^- - \mathbf{q}_\perp^2 = -Q^2$ , i.e.  $Q^2 > 0$  is spacelike momentum transfer.

The matrix element of the current given by Eq. (5) can be expressed as a convolution integral in terms of LF wave function,  $\Psi^s(x, \mathbf{k}_\perp)$  as shown in Fig. 1:

$$\begin{aligned} \langle P' | J^\mu(0) | P \rangle &= \sum_{\lambda_q \lambda'_q \lambda_{\bar{q}}} \int_0^1 dx \int d^2 \mathbf{k}_\perp \Psi_{\lambda'_q \lambda_{\bar{q}}}^{s*}(x, \mathbf{k}'_\perp) \\ &\times \frac{\bar{u}_{\lambda'_q}(p'_q)}{\sqrt{p_q^+}} \Gamma^\mu \frac{u_{\lambda_q}(p_q)}{\sqrt{p_q^+}} \Psi_{\lambda_q \lambda_{\bar{q}}}^s(x, \mathbf{k}_\perp), \end{aligned} \quad (6)$$

where  $p_q^+ = p_q'^+ = (1-x)P^+$  and  $\mathbf{k}'_\perp = \mathbf{k}_\perp - x\mathbf{q}_\perp$  in the initial pion rest frame,  $\mathbf{P}_\perp = 0$ . The helicity of the quark(antiquark) is denoted as  $\lambda_{q(\bar{q})}$ . Since the matrix element of the current in Eq. (6) is symmetric under the exchange of  $q$  and  $\bar{q}$ , we do not explicitly write the contribution of photon-antiquark interaction diagram as well as the charge factor.

Our LF wave function  $\Psi^s$  in Eq. (6) is given by

$$\Psi_{\lambda_q \lambda_{\bar{q}}}^s(x, \mathbf{k}_\perp) = \sqrt{\frac{\partial k_z}{\partial x}} \Phi(x, \mathbf{k}_\perp) \mathcal{R}_{\lambda_q \lambda_{\bar{q}}}(x, \mathbf{k}_\perp), \quad (7)$$

where  $\Phi$  and  $\mathcal{R}$  are the radial and relativistic spin-orbit wave functions, respectively. Our radial wave function is given by the gaussian trial function for the variational principle to the QCD-motivated effective LF Hamiltonian [12]:

$$\Phi(\mathbf{k}^2) = \left(\frac{1}{\pi^{3/2} \beta^3}\right)^{1/2} \exp(-\mathbf{k}^2/2\beta^2), \quad (8)$$

where  $\mathbf{k} = (k_z, \mathbf{k}_\perp)$  is three vector and  $\Phi(\mathbf{k}^2)$  satisfies  $\int d^3 k |\Phi(\mathbf{k}^2)|^2 = 1$ . The LF variable  $(x, \mathbf{k}_\perp)$  is introduced in Eq. (8) by the definition of the longitudinal momentum  $k_z$  via  $k_z = (x - 1/2)M_0$  with  $M_0^2 = (m^2 + \mathbf{k}_\perp^2)/x(1-x)$ . If the quark mass depends on  $x$  and  $\mathbf{k}_\perp$ , the Jacobian of the variable transformation  $(k_z, \mathbf{k}_\perp) \rightarrow (x, \mathbf{k}_\perp)$  in Eq. (7) is obtained as

$$\frac{\partial k_z}{\partial x} = \frac{M_0}{4x(1-x)} + \frac{(2x-1)m(x, \mathbf{k}_\perp)}{2x(1-x)M_0} \frac{\partial m(x, \mathbf{k}_\perp)}{\partial x}. \quad (9)$$

The spin-orbit wave function for a pseudoscalar meson ( $J^{PC} = 0^{-+}$ ) is obtained [10,12] by the interaction independent Melosh transformation as follows:

$$\mathcal{R}_{\lambda_q \lambda_{\bar{q}}}(p_q, p_{\bar{q}}) = \frac{\bar{u}(p_q, \lambda_q) \gamma_5 v(p_{\bar{q}}, \lambda_{\bar{q}})}{\sqrt{2}M_0}. \quad (10)$$

### III. QUARK MASS EVOLUTION AND LOCAL GAUGE INVARIANCE

The solution of the DSE for the renormalized dressed-quark propagator takes the form in Minkowski space

$$S(p)^{-1} = A(p^2)\not{p} - B(p^2), \quad (11)$$

where the quark mass evolution function  $m(p^2)$  is defined as  $m(p^2) = B(p^2)/A(p^2)$ . Also, the gauge invariance requires that the quark-photon vertex  $\Gamma^\mu$  given by Eq. (6) satisfy the vector Ward-Takahashi identity (WTI) [19] (i.e. current conservation)

$$-q^\mu \Gamma_\mu(p; q) = S(p')^{-1} - S(p)^{-1}, \quad (12)$$

where  $q = p - p'$ . At zero momentum transfer  $q=0$ , the quark-photon vertex is also specified by the differential Ward identity (i.e. charge conservation)  $\Gamma^\mu(p; 0) = \partial S(p)^{-1}/\partial p_\mu$ . The bare quark-photon vertex,  $\Gamma^\mu = \gamma^\mu$ , which is usually used in LFCQM [10–12], is inadequate when the quark propagator has momentum-dependent dressing because it violates WTI. As used in many DSE studies of EM interactions [21,14], we take the Ball-Chiu(BC) ansatz [22] for the quark-photon vertex

$$\begin{aligned} \Gamma_{\text{BC}}^\mu &= \frac{(\not{p} + \not{p}')}{2} (p + p')^\mu \frac{A(p'^2) - A(p^2)}{p'^2 - p^2} \\ &+ \frac{A(p'^2) + A(p^2)}{2} \gamma^\mu - (p + p')^\mu \frac{B(p'^2) - B(p^2)}{p'^2 - p^2}. \end{aligned} \quad (13)$$

Here, we introduce two algebraic parametrizations of the quark running mass, i.e. crossing asymmetric(CA) and crossing symmetric(CS) mass functions proportional to  $p^2$  and  $p^4$ , respectively. For the CA mass evolution function, we take

$$m(p^2) = m_0 + (m_c - m_0) \frac{1 + \exp(-\mu^2/\lambda^2)}{1 + \exp[(-p^2 - \mu^2)/\lambda^2]}, \quad (14)$$

where  $m_0$  and  $m_c$  are the current and constituent quark masses, respectively. The parameters  $\mu$  and  $\lambda$  are used to adjust the shape of the mass evolution. Similarly, the following form of the mass evolution function is used for the CS case

$$m(p^4) = m_0 + (m_c - m_0) \frac{1 + \exp(-\mu^4/\lambda^4)}{1 + \exp[(p^4 - \mu^4)/\lambda^4]}, \quad (15)$$

where we simply replace  $-p^2$  and  $\mu^2(\lambda^2)$  in Eq. (14) with  $p^4$  and  $\mu^4(\lambda^4)$ , respectively. In our case, we set  $A(p^2)=1$ ,  $B(p^2)=m(p^2)$  for CA and  $B(p^2)=m(p^4)$  for the CS case, respectively. While Eqs. (14) and (15) are phenomenological, the results of our running mass in spacelike momentum region ( $-p^2 > 0$ ) yield a generic picture of the quark mass evolution from the low energy limit of the constituent quark mass to the high energy limit of the current quark mass. For comparison, we use in Fig. 2 two different parameter sets for each mass evolution function, i.e.,  $(\mu^2, \lambda^2) = (0.9, 0.2)$  [Set 1] and  $(0.5, 0.2)$  [Set 2] (in unit of GeV<sup>2</sup>) for  $m(p^2)$  and  $(\mu^2, \lambda^2) = (0.95, 0.63)$  [Set 1] and  $(0.28, 0.55)$  [Set 2] (in unit of GeV<sup>2</sup>) for  $m(p^4)$ , respectively (See Fig. 2 for the line code). The current and constituent quark masses used are  $m_0 = 5$  MeV

and  $m_c = 220$  MeV, respectively. Simulating the constituent picture at small momentum region, we have chosen these particular sets of parameters, [Set 1] and [Set 2] for each mass function, to keep the constituent mass up to  $(-p^2) \sim 1$  and  $0.5$  GeV<sup>2</sup>, respectively, before it drops exponentially.

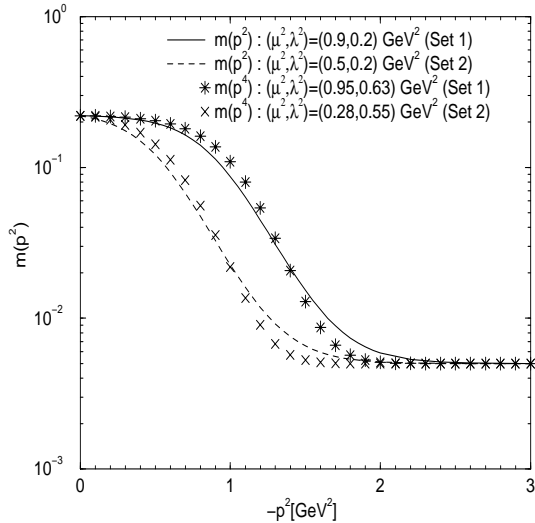


FIG. 2. Quark mass evolution in spacelike momentum region,  $-p^2 > 0$ .

In order to express the four momentum  $p^2$  in terms of LF variables  $(x, \mathbf{k}_\perp)$ , we use the on-mass shell condition,  $p^2 = m^2(p^2)$ . It implies zero binding energy of a mock meson, i.e.  $P^- = p_q^- + p_{\bar{q}}^-$  where  $P^- (= P^0 - P^3)$  and  $p_q^- (p_{\bar{q}}^-)$  are the LF energies of the mock meson and the quark(antiquark), respectively. It leads to the following identity for the pion case ( $m_q = m_{\bar{q}}$ )

$$p^2 = x(1-x)\tilde{M}^2 - \mathbf{k}_\perp^2. \quad (16)$$

For the mock meson mass  $\tilde{M}$ , we take the average value(so called spin-averaged meson mass) of  $\pi(m_\pi)$  and  $\rho(m_\rho)$  masses with appropriate weighting factors from the spin degrees of freedom, i.e.  $\tilde{M} = (m_\pi + 3m_\rho)_{\text{exp}}/4 = 612$  MeV, which is consistent with quark model calculations with typical constituent quark masses and been used in some constituent LFQM calculations [11]. Note that the spacelike form factor  $F_\pi(Q^2)$  is weakly dependent on  $\tilde{M}$ , i.e. the numerical result with the mock meson mass  $\tilde{M} = 612$  MeV is not much different from that with the physical pion mass  $m_\pi = 140$  MeV, which would be used in the LFBS-LFDS approach. Using Eq. (16), we can now express the mass evolution functions  $m(p^2)$  and  $m(p^4)$  in terms of LF variables  $x$  and  $\mathbf{k}_\perp$ .

Using the good component of the current,  $J^+$ , the pion EM form factor in Eq. (5) is obtained as

$$F_\pi(Q^2) = N_\pi \int dx d^2\mathbf{k}_\perp \sqrt{\frac{\partial k'_z}{\partial x}} \sqrt{\frac{\partial k_z}{\partial x}} \Phi_f^*(x, \mathbf{k}'_\perp) \Phi_i(x, \mathbf{k}_\perp) \times \left\{ \frac{\mathbf{k}_\perp \cdot \mathbf{k}'_\perp + m_k m_{k'}}{x(1-x)M_0 M'_0} + \frac{m_k \Delta m_k (2\tilde{M}^2 + \mathbf{q}_\perp^2)}{M_0 M'_0 \Delta \mathbf{k}_\perp^2} \right\}, \quad (17)$$

where  $N_\pi$  is the normalization constant and  $\Delta m_k = m(x, \mathbf{k}'_\perp) - m(x, \mathbf{k}_\perp) = m_{k'} - m_k$  and  $\Delta \mathbf{k}_\perp^2 = \mathbf{k}'_\perp^2 - \mathbf{k}_\perp^2$ . The other primed terms,  $k'_z$  and  $M'_0$ , are obtained from  $k_z(x, \mathbf{k}_\perp \rightarrow \mathbf{k}'_\perp)$  and  $M_0(x, \mathbf{k}_\perp \rightarrow \mathbf{k}'_\perp)$ , respectively. The terms in the curly bracket are obtained from the trace of spin-orbit wave function, i.e.  $\sum \mathcal{R}^\dagger(\bar{u}/\sqrt{p_q^+}) \Gamma_{\text{BC}}^+(u/\sqrt{p_q^+}) \mathcal{R}$ . Note that the normalization constant  $N_\pi$  at  $Q^2 = 0$  is exactly one in chiral limit ( $m_0 = \tilde{M} = 0$ ).

We also obtain the quark condensate from the PCAC relation given by Eq. (1) as follows:

$$\langle \bar{q}q \rangle = -\frac{f_\pi \sqrt{N_c}}{(2\pi)^{3/2}} \int \frac{dx d^2\mathbf{k}_\perp}{x(1-x)} \sqrt{\frac{\partial k_z}{\partial x}} \Phi(x, \mathbf{k}_\perp) \sqrt{m_k^2 + \mathbf{k}_\perp^2}, \quad (18)$$

where  $N_c=3$  is the color factor. This is equivalent to the expression in DS models [14] for  $A(p^2) = 1$ . The quark condensate is normally evaluated at the spacelike momentum scale  $p \sim 1$  GeV (corresponding to the renormalization point  $\nu$  [14]) where  $m_k \rightarrow m_0$  (see Fig. 2).

#### IV. NUMERICAL RESULTS

In our numerical calculations, we use the model parameters  $(m_c, \beta) = (0.22, 0.3659)$  [GeV] obtained in Ref. [12] for the linear confining potential model where the charge radius ( $r_\pi^2 = -6dF_\pi(Q^2)/dQ^2|_{Q^2=0}$ ) and decay constant ( $\langle 0|\bar{q}\gamma^\mu\gamma_5 q|P \rangle = i f_\pi P^\mu$ ) of the pion were predicted as  $r_\pi^2 = 0.425$  [fm<sup>2</sup>] (Exp. =  $0.432 \pm 0.016$  [23]) and  $f_\pi = 130$  MeV (Exp. =  $131$  MeV [24]), respectively. The change of the charge radius and decay constant from the CQM result due to the running mass formulae are within 2% and 5%, respectively. For the calculation of the quark condensate, we obtain, for example,  $f_\pi = 127$  MeV from the [Set 1] of the CA mass function. Consequently, we obtain from Eqs. (1) and (18) the pion mass and the quark condensate as  $m_\pi = 164$  MeV and  $-\langle \bar{q}q \rangle = (0.3 \text{ GeV})^3$  while the experimental values of  $m_\pi$  and  $-\langle \bar{q}q \rangle$  are  $140$  MeV and  $(0.236 \text{ GeV})^3$  [25], respectively. This shows the PCAC relation is reasonably well satisfied in LFQM with our mass evolution function. The results from other parameter sets are not much different from the above [Set 1] of CA case.

In Fig. 3, we show our results of the pion EM form factor for small  $Q^2$  region using the [Set 2] with BC vertex for both CA and CS mass evolution functions and compare with the experimental data [23] as well as the CQM result given by Ref. [12]. The line code is in the

figure. The small momentum( $Q^2$ ) behavior of the form factor with CA and CS mass functions are not only close to each other but also close to the experimental data [23] as well as the CQM result [12]. The results of [Set 1] for both CA and CS mass functions are even closer to the CQM result.

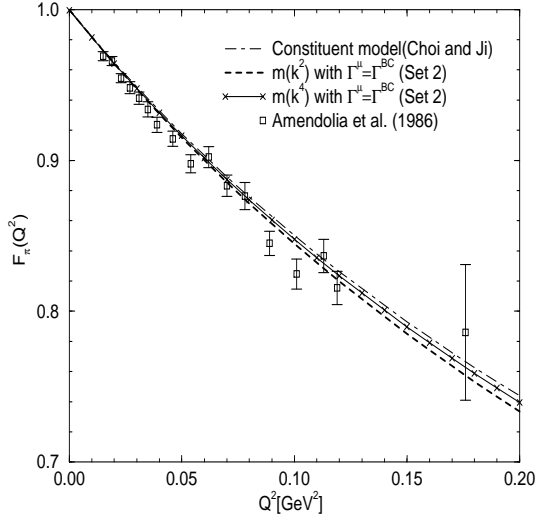


FIG. 3. Pion EM form factor for small  $Q^2$  region using the [Set 2] for both CA and CS mass formulae compared with the experimental data [23] and the CQM result [12].

We also show in Fig. 4 our results of the form factor for the intermediate  $Q^2$  region for CA [Fig. 4(a)] and CS [Fig. 4(b)] mass functions compared with the experimental data [7,26] as well as the CQM result [12]. The line code is given in each figure. As one can see from Fig. 4, (1) the difference between the bare vertex and BC ansatz indicates the breakdown of the local gauge invariance from the usage of the bare vertex, (2) the [Set 2] for both CA and CS mass functions show larger deviation from the CQM result than the [Set 1] case for the momentum transfer  $Q^2 \sim 2 \text{ GeV}^2$  and above region, (3) the results with BC vertex fall off faster (at around  $Q^2=2 \text{ GeV}^2$ ) than the CQM result does, (4) the mass evolution effects from [Set 1] for both CA and CS cases are not much different from the constituent result up to  $Q^2=8 \text{ GeV}^2$ , and (5) the CA mass evolution function is more sensitive to the variation of the momentum dependence than the CS mass evolution function.

## V. CONCLUSION

In conclusion, we have reexamined the soft contribution to the pion elastic form factor in the framework of the LFBS with a  $Q^2$ -dependent quark mass that could be obtained from a LFDSE. This is equivalent to the LFQM with a running quark mass. The Ball-Chiu ansatz was

used for the dressed quark-photon vertex. We showed that the PCAC relation in Eq. (1) is satisfied in LFQM with our running mass formulae. The CQM result is not affected too much by the quark mass evolution for the small momentum transfer region up to  $Q^2=1\sim 2 \text{ GeV}^2$ .

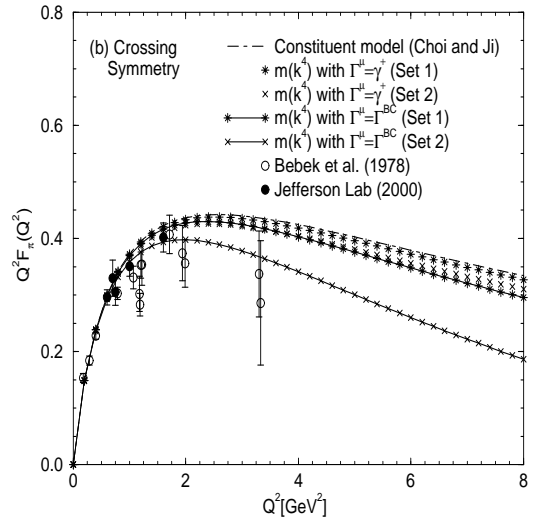
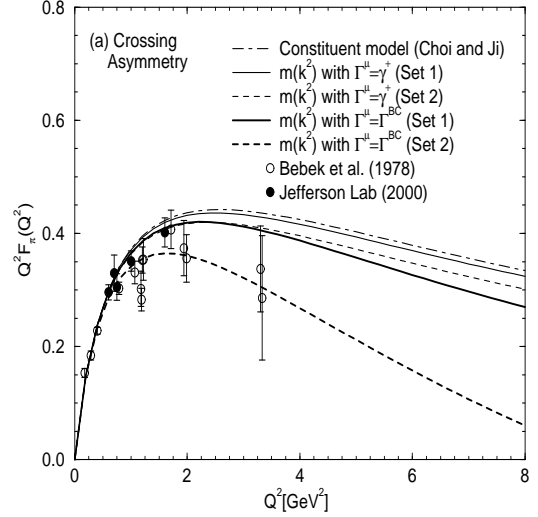


FIG. 4. Pion EM form factor:(a) Crossing asymmetry(CA) and (b) Crossing symmetry(CS) mass functions compared with the experimental data [7,26] as well as the CQM result [12].

However, the form factor is sensitive to the shape of the mass evolution for the intermediate ranges, e.g. the [Set 1] for both CA and CS cases are not much different from the LFQM result but the [Set 2] show a sizable effect on the soft pion elastic form factor for  $Q^2 \sim 2 \text{ GeV}^2$  and above. It may be interesting to observe from [Set 2] that the form factor may distinguish the mass evolu-

tion respecting CS from the one not respecting CS even though they show similar momentum dependent behavior as shown in Fig. 2. While our calculation employed a phenomenological mass evolution functions and the quark-photon vertex modification, the qualitative feature presented in this work might not be significantly modified even if one were to use the more realistic solutions obtained from the first principle. However, it may be interesting to check further whether the soft part would fall more rapidly if the present results of DS [14] and LFDS [18] models were used. The “hard-scattering” contribution to the pion form factor, i.e. the second term in Eq. (4), is under investigation.

### Acknowledgements

The authors would like to acknowledge helpful discussions with Otto Linsuain and Pieter Maris. The work of L.S.K. and H-M.C was supported in part by the NSF grant PHY-00070888 and that of C-R. Ji by the US DOE under grant No. DE-FG02-96ER40947. The North Carolina Supercomputing Center and the National Energy Research Scientific Computer Center are also acknowledged for the grant of Cray time.

- [12] H.-M. Choi and C.-R. Ji, Phys. Rev. D **59**, 074015 (1999).
- [13] S. D. Drell and T. M. Yan, Phys. Rev. Lett. **24**, 181 (1970); G. West, Phys. Rev. Lett. **24**, 1206 (1970).
- [14] C. D. Roberts and A. G. Williams, Prog. Part. Nucl. Phys. **33**, 477 (1994); P. C. Tandy, Prog. Part. Nucl. Phys. **39**, 117 (1997); P. Maris and C. D. Roberts, Phys. Rev. C **58**, 3659 (1998).
- [15] L.S. Kisslinger and T. Meissner, Phys. Rev. C **57**, 1528 (1998).
- [16] T. Meissner and L.S. Kisslinger, Phys. Rev. C **59**, 986 (1999).
- [17] P. Maris and P.C. Tandy, Phys. Rev. C **61**, 045202 (2000).
- [18] L.S. Kisslinger and O. Linsuain, in preparation.
- [19] J. C. Ward, Phys. Rev. **78**, 182 (1950); Y. Takahashi, Nuovo Cimento **6**, 371 (1957).
- [20] C. -R. Ji and H. -M. Choi, hep-ph/0009281.
- [21] P. Maris, C. D. Roberts, and P. C. Tandy, Phys. Lett. B **420**, 267 (1998).
- [22] J.S. Ball and T.-W. Chiu, Phys. Rev. D **22**, 2542 (1980).
- [23] R. A. Amendolia et al., Phys. Lett. B **178**, 435 (1986).
- [24] Particle Data Group, D. E. Groom et al., Eur. Phys. J. C **15**, 1 (2000).
- [25] D. B. Leinweber, Ann. Phys. (N. Y.) **254**, 328 (1997).
- [26] C. J. Bebek et al., Phys. Rev. D **17**, 1693 (1978).

- 
- [1] V.L. Chernyak and A.R. Zhitnitsky, Phys. Rep. **112**, 173 (1984); N. Isgur and C.H. Lewellyn-Smith, Phys. Rev. Lett. **52**, 1080 (1984); S. J. Brodsky, C.-R. Ji, A. Pang and D. Robertson, Phys. Rev. D **57**, 245 (1998); A. Szczepaniak, C.-R. Ji and A. Radyushkin, Phys. Rev. D **57**, 2813 (1998).
  - [2] S. J. Brodsky, H.-C. Pauli, and S. S. Pinsky, Phys. Rept. **301**, 299(1998).
  - [3] O.C. Jacob and L.S. Kisslinger, Phys. Rev. Lett. **56**, 225 (1986); Phys. Lett. B **243**, 323 (1990).
  - [4] G. P. Lepage and S. J. Brodsky, Phys. Rev. D **22**, 2157 (1980).
  - [5] L.S. Kisslinger and S.W. Wang, hep-ph/9403261; Nucl. Phys. B **399**, 63 (1993).
  - [6] V.V. Sudakov, Sov. Phys. JETP **3**, 65 (1956).
  - [7] J. Volmer et al., nucl-ex/0010009.
  - [8] M. Gell-Mann, R.J. Oakes and B. Renner, Phys. Rev. **175**, 2195 (1968).
  - [9] P.M Dirac, Rev. Mod. Phys. **21**, 392 (1949).
  - [10] P. L. Chung, F. Coester, and W. N. Polyzou, Phys. Lett. B **205**, 545 (1988); W. Jaus, Phys. Rev. D **44**, 2851 (1991); F. Cardarelli et al., Phys. Rev. D **53**, 6682 (1996); H.-M. Choi and C.-R. Ji, Phys. Rev. D **56**, 6010 (1997).
  - [11] Z. Dziembowsky and L. Mankiewicz, Phys. Rev. Lett. **58**, 2175 (1987); Z. Dziembowsky, Phys. Rev. D **37**, 778 (1988); C.-R. Ji and S. R. Cotanch, Phys. Rev. D **41**, 2319 (1990); H.-M. Choi and C.-R. Ji, Nucl. Phys. A **618**, 291 (1997).